

18. R. M. Story and T. A. Steitz, *J. Mol. Biol.* **355**, 374 (1992).
19. R. C. Benedict and S. C. Kowalczykowski, *J. Biol. Chem.* **263**, 5450 (1991).
20. S. Tateishi, T. Horii, T. Ogawa, H. Ogawa, *J. Mol. Biol.* **223**, 115 (1992).
21. B. Lee and F. M. Richards, *ibid.* **55**, 379 (1971).
22. R. M. Story and D. K. Bishop, data not shown.
23. D. Bashford, C. Chothia and A. M. Lesk, *J. Mol. Biol.* **196**, 199 (1987).
24. L. T. J. Delbaere, W. L. B. Hutcheon, M. N. G. James, W. E. Thiessen, *Nature* **257**, 758 (1975).
25. L. A. Kohlstaedt, J. Wang, J. M. Friedman, P. A. Rice, T. A. Steitz, *Science* **256**, 1783 (1992).
26. M. Delarue, O. Poch, N. Tordo, D. Moras, P. Argos, *Protein Eng.* **3**, 461 (1990).
27. T. Ogawa, X. Yu, A. Shinohara, E. H. Egelman, *Science* **259**, 1896 (1993).
28. T. Kodadek and B. M. Alberts, *Nature* **326**, 312 (1987).
29. L. D. Harris and J. D. Griffith, *J. Mol. Biol.* **206**, 19 (1989).
30. T. Formosa and B. M. Alberts, *Cell* **47**, 793 (1986).
31. T. Kodadek, D. C. Gan, K. Sternke-Hale, *J. Biol. Chem.* **264**, 16451 (1989).
32. J. W. Little, *Proc. Natl. Acad. Sci. U.S.A.* **81**, 1375 (1984).
33. S. E. Burckhardt, R. Woodgate, R. H. Sheer-mann, H. Echols, *ibid.* **85**, 1811 (1988).
34. J. E. Walker, M. Saraste, M. J. Runswick, N. J. Gay, *EMBO J.* **1**, 945 (1982).
35. A. I. Roca and M. M. Cox, personal communication.
36. A. McLachlan, *J. Mol. Biol.* **61**, 409 (1971).
37. We thank A. I. Roca and M. M. Cox for kindly providing an unpublished comparison of bacterial RecA sequences. This work was supported in part by NIH grant GM22778 to T.A.S.

8 January 1993; accepted 5 March 1993

Similarity of the Yeast RAD51 Filament to the Bacterial RecA Filament

Tomoko Ogawa, Xiong Yu, Akira Shinohara, Edward H. Egelman*

The RAD51 protein functions in the processes of DNA repair and in mitotic and meiotic genetic recombination in the yeast *Saccharomyces cerevisiae*. The protein has adenosine triphosphate-dependent DNA binding activities similar to those of the *Escherichia coli* RecA protein, and the two proteins have 30 percent sequence homology. RAD51 polymerized on double-stranded DNA to form a helical filament nearly identical in low-resolution, three-dimensional structure to that formed by RecA. Like RecA, RAD51 also appears to force DNA into a conformation of approximately a 5.1-angstrom rise per base pair and 18.6 base pairs per turn. As in other protein families, its structural conservation appears to be stronger than its sequence conservation. Both the structure of the protein polymer formed by RecA and the DNA conformation induced by RecA appear to be general properties of a class of recombination proteins found in prokaryotes as well as eukaryotes.

The RecA protein of *E. coli* is the most intensively studied enzyme involved in genetic recombination (1-4). In the presence of adenosine triphosphate (ATP) or an ATP analog, RecA can polymerize on single- or double-stranded DNA to form a helical nucleoprotein filament with about 6.2 RecA protomers per filament turn and a pitch of approximately 92 to 97 Å (5). Within this filament, both double-stranded DNA (dsDNA) and single-stranded DNA (ssDNA) are extensively stretched and dsDNA is unwound. The active form of RecA as determined by adenosine triphosphatase (ATPase) activity, strand-exchange activity, and the cleavage of the LexA and phage repressors exists only in this extended filament. We now show that the RAD51 protein from the yeast *S. cerevisiae*, which functions in DNA repair and recombination (6), induces a similar conformation in

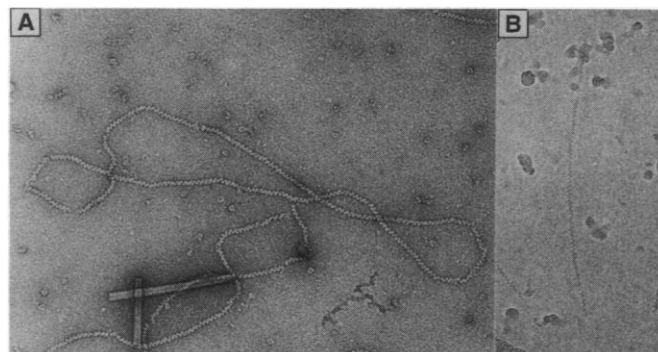
DNA and forms helical nucleoprotein filaments similar to those formed by RecA.

When cloned and purified from *E. coli*, RAD51 has ATP-dependent DNA binding activities similar to those of RecA (6). The

RAD51 protein contains 400 amino acid residues. Within a 221-residue core region, 30% of the residues are identical and 24% are similar to those of the corresponding region of *E. coli* RecA (6). Thus, 119 out of 400 residues, or 30% of the total sequence of RAD51, are either identical or similar to those of RecA. We have purified RAD51 from *S. cerevisiae* to 95% purity (7). In the presence of ATP, this protein forms filaments on dsDNA that are similar to the filaments formed by RecA protein (Fig. 1). After covering circular dsDNA molecules with RAD51, we measured the extension of the DNA induced by RAD51. The DNA was greatly extended from a 3.4 Å rise per base pair found in B-DNA to an axial rise per base pair of 5.1 Å (Fig. 2). This extension of DNA is the same as that induced by RecA protein (8).

Fourier transforms of filament images were used to determine the pitch of the RAD51-ATP-DNA filament from both negatively stained and frozen-hydrated filaments (Fig. 3). The mean pitch of 99 Å is greater than that of comparable RecA-ATP-DNA filaments, which have a mean pitch of about 92 Å. Fourier transforms of such filaments also revealed that these filaments have a helical symmetry nearly identical to that of RecA-ATP-DNA filaments. This helical symmetry made it possible to generate three-dimensional reconstructions from single views of individual filaments (9). Negatively stained filaments were used for the reconstruction rather than frozen-hydrated filaments for several reasons. (i) There was no detectable change of pitch as a result of dehydration with the negative staining (Fig. 3). (ii) We found no evidence that the frozen-hydrated filaments were better preserved than the negatively stained. (iii) In the frozen-hydrated filaments, weak contrast and a poor signal-to-

Fig. 1. Electron micrographs of RAD51 protein polymerized on DNA. (A) Negatively stained filaments of RAD51 on circular ΦX174 dsDNA observed by conventional transmission electron microscopy. (B) Unstained, frozen-hydrated RAD51 filament on linear dsDNA observed by cryo-electron microscopy (28). Under the conditions used (29), RAD51 protein (unlike RecA protein) does not form filaments on ssDNA with ATP or on dsDNA with the slowly hydrolyzable ATP analog ATP-γ-S (30). This may explain the inability of RAD51 to catalyze ssDNA-dsDNA strand-exchange reactions because although RAD51 has a ssDNA-dependent ATPase activity (7), the RecA-catalyzed ssDNA-dsDNA exchange reaction proceeds by way of the formation of the active filament on ssDNA, and RAD51 fails to form filaments on ssDNA. The tobacco mosaic viruses seen in (A) are about 200 Å in diameter, and both micrographs are shown at the same magnification.



T. Ogawa and A. Shinohara, Department of Biology, Osaka University, Osaka 560, Japan.
X. Yu and E. H. Egelman, Department of Cell Biology and Neuroanatomy, University of Minnesota Medical School, Minneapolis, MN 55455.

*To whom correspondence should be addressed.

noise ratio made the additional layer lines more difficult to see. (iv) In the negatively stained filaments, the contrast transfer function could be ignored.

The Fourier transform of the projection of a helical object is nonzero everywhere except on layer lines, where the spacing of the layer lines is reciprocally related to the pitch of the helices from which they arise. After 120 filaments were digitized, straightened (10), and Fourier-transformed, 20 filaments were found with layer lines in addition to the strong layer line at $1/(99 \text{ \AA})$ that arises from the one-start helix. After several cycles of averaging, 17 filaments were found

to average well together, and these data were used for the reconstruction (Fig. 4). The average symmetry (\pm SD) of the 17 filaments was 6.18 ± 0.04 subunits per turn of the 99 \AA pitch helix. The rise per RAD51 subunit in these filaments was therefore about 16 \AA . Because the rise per base pair was about 5.1 \AA , the stoichiometry is quite consistent with the three base pairs per subunit observed in RecA filaments (11). For the DNA to be bound along the helical path of the RAD51 protein, the DNA must be untwisted so that there are about 3×6.2 (or 18.6) base pairs per helical turn of the DNA. This amount of untwisting

of DNA has been directly measured for the RecA-DNA complex (12).

A three-dimensional reconstruction of the RAD51-ATP-dsDNA complex (Fig. 4A) shows that when the filaments are formed under conditions similar to those used for the RecA reconstruction (13) (Fig. 4B), filaments of RAD51 and RecA are quite similar. A comparison of the two suggests that the RAD51 filament is less regular than the flexible RecA filament. A comparison of layer line data suggests that the resolution of the RAD51 reconstruction is lower than that of the comparable RecA reconstruction. Because a crystal structure exists for the RecA protein (14), the low-resolution reconstruction of the RAD51 protein was directly related to an atomic model for RecA. Several factors were considered in this comparison, however. A comparison between the active, 95 \AA pitch RecA-DNA-ATP filament and the 83 \AA pitch RecA crystal structure (14) was complicated because the RecA crystal structure contains no DNA and no nucleotide. As a result, RecA within the crystal appears to be similar in structure to the inactive, 75 \AA pitch RecA filament formed with or without DNA in the absence of a nucleotide cofactor (15).

The RecA filament has a deep helical groove with subunits arranged so that one side of the groove is relatively smooth, whereas subunits protrude into the groove on the other side in a pendulous manner. Much larger subunit lobes are present in the crystal structure than in an averaged RecA data set, but an early reconstruction from a single RecA filament (16) displays larger subunit lobes more similar to those of the crystal. A likely explanation is that these lobes may be quite disordered in RecA and thus are not visualized after extensive averaging.

The RAD51 filaments appear less regular than the RecA filaments, and the lobes of the RAD51 subunits are even less visible. However, the main lobe seen in the RecA crystal arises from residues 270 to 328, whereas the RAD51 protein terminates at approximately residue 266 of RecA when it is aligned against the RecA sequence (6). After truncation at residue 266, the match of the RecA crystal structure to the RAD51 reconstruction was greatly improved (Fig. 4, D and H). Thus, the failure to see lobes in RAD51 reflects a genuine structural difference with RecA and not disorder. The DMC1 protein of yeast (17), which is homologous to both RecA and RAD51, is also terminated at about residue 266 of RecA when aligned against the RecA sequence. Although RAD51 has approximately 120 additional NH_2 -terminal residues not present in RecA, it does not show any additional density regions in the reconstruction that are not present in RecA. We can eliminate the possibility that this region is proteolyti-

Fig. 2. The contour length of nicked circular Φ X174 dsDNA covered with the RAD51 protein (bottom scale). For the number of base pairs per molecule (5386), the contour length can be directly converted to the axial rise per base pair (top scale). Conditions were as described (29). Electron micrographs of negatively stained specimens were recorded at $\times 30,000$ magnification and enlarged approximately 2.5-fold. A digitizing tablet was used to trace the contours of the circles from the prints. For B-DNA, the axial rise per base pair is 3.4 \AA , which is equivalent to a contour length of 1.8 \mu m . This contour length is significantly smaller than any measured. Inspection of electron micrographs (Fig. 1A) shows small gaps and kinks in the RAD51-covered circles, possibly arising from multiple nucleation points around the circle. Under similar conditions, the RecA protein would nucleate less frequently and would therefore form more continuous polymers. Thus, we expected that most of the circles would have contour lengths less than maximal extension as a result of the incomplete saturation of the DNA by RAD51 and that this could result in an asymmetrical distribution of contour lengths with a tail extending to smaller values. This is exactly what was observed. The maximal extension that we measured is indicated by the arrow, which corresponds to the previously determined rise per base pair of 5.1 \AA in RecA-DNA-ATP- γ -S filaments (8).

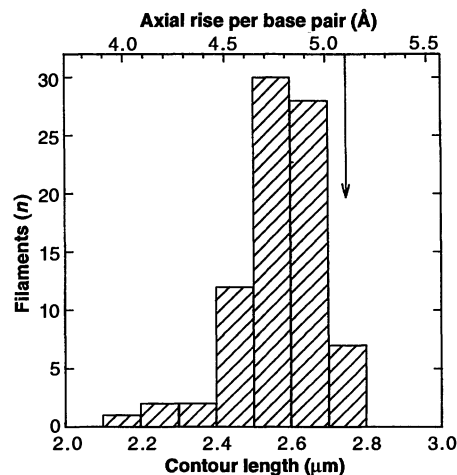


Fig. 3. The helical pitch of RAD51 protein filaments formed on dsDNA (A and B) and of RecA filaments on dsDNA under comparable conditions (C). Both the RAD51 and RecA filaments were prepared with ATP and then stabilized with AlF_4^- (29). Data are from both negatively stained filaments [(A) and (C)] and frozen-hydrated filaments (B), and there is little shift in the distributions between these two techniques for filaments in this state. For inactive RecA filaments formed on DNA in the absence of a nucleotide cofactor, there is compression of filaments induced by dehydration during negative stain preparation (15, 31, 32). There is a clear shift in pitch between the RecA filaments and the RAD51 filaments. The means and SDs are as follows: (A), $98.9 \pm 1.4 \text{ \AA}$; (B), $98.8 \pm 2.0 \text{ \AA}$; and (C), $92.1 \pm 1.6 \text{ \AA}$. All filaments were formed on linear DNA, the images of filament sections were straightened (10) and Fourier-transformed, and the position of the layer line arising from the one-start helix was used to determine the mean pitch for each section. The length of section used was typically about 2500 \AA , except for the frozen-hydrated RAD51 filaments (B), in which sections were typically about 1500 \AA in length. The short lengths of the RAD51 filaments (the relatively long one shown in Fig. 1B is about 0.6 \mu m long) eliminates the flow-induced stretching of long (2 to 3 \mu m) RecA filaments that can be observed in ice (15). The 23 \AA pitch of tobacco mosaic virus, coprepared with both RAD51 and RecA, was used to determine the absolute scale. The data in (C) are from Yu and Egelman (13).

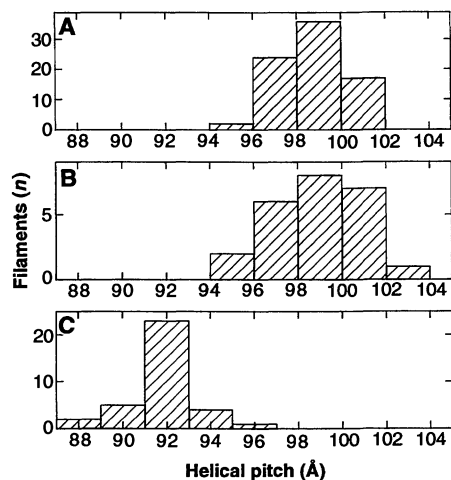
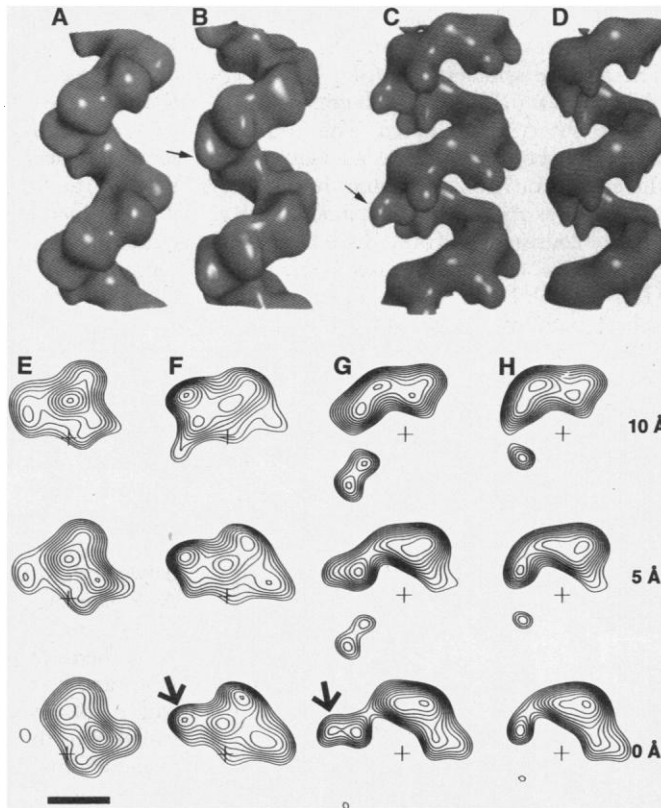


Fig. 4. A three-dimensional reconstruction of the RAD51-ATP-dsDNA filament (**A** and **E**) and, for comparison, a RecA-ATP-dsDNA reconstruction (13) (**B** and **F**); Low-resolution renderings of the RecA crystal (14) (**C**, **D**, **G**, and **H**). Surface views are shown in (**A**) to (**D**), whereas contour plots of cross sections, cut perpendicular to the filament axis, are shown in (**E**) to (**H**). The cross sections are from axial levels of 0, 5, and 10 Å within the filament, and the helical axis is marked by a cross in each of the sections. The RAD51 filaments were prepared on linear dsDNA and negatively stained (29) and reconstructed as described (33). The RecA reconstruction (**B**) is shown with the 3' end at the bottom (34), and the RAD51 reconstruction is shown oriented with the polarity that gives the best agreement with the RecA reconstruction. The main difference seen in the surface views is the additional mass attributable to the "lobes" of the subunit, which protrude into the helical groove and which can be seen in the RecA reconstruction [arrow in (**B**) and (**F**)] but not in the RAD51 reconstruction. The 83 Å pitch RecA crystal filament is shown in (**C**) and (**G**), whereas a truncated version, missing all COOH-terminal residues beyond residue 266, is shown in (**D**) and (**H**). The arrow in (**C**) and (**G**) indicates the outer lobe generated by RecA residues 266 through 328 in the crystal structure. The RAD51 protein terminates at residue 266 of the RecA sequence when the two protein sequences are aligned (6); the match of the RecA crystal structure to RAD51 is greatly improved with the elimination of the RecA outer lobe. The scale bar in (**E**) is 40 Å.



cally cleaved because gels run both before and after polymerization are consistent with the 43-kD molecular size. Thus, the helically averaged reconstruction of RAD51 shows the more rigid helical core that exists in common with RecA, whereas part of the protein (the NH₂-terminus) may exist as a highly flexible domain and is not visualized after helical averaging.

The function of the COOH-terminal residues that are present in RecA but absent in RAD51 and DMC1 is not entirely clear. Story *et al.* (14) have suggested that a part of this COOH-terminus in RecA is involved in filament-filament interactions within the cell that maintain RecA in an inactive storage form. Although basal levels of RecA must exist in the cell before SOS induction in order to cleave the LexA repressor, there is no evidence for any corresponding role for RAD51. In vitro studies have shown that RecA proteins missing the COOH-terminal 20 to 45 residues are still capable of initiating strand-exchange reactions and stimulating LexA repressor cleavage (18–20). A structural

study suggests that the removal of 18 residues from the RecA COOH-terminus results in a conformational change visible at low resolution (21). In addition, truncated RecA genes ending between residues 203 to 290 suppress *in vivo* recombination when expressed in cells that contain the wild-type RecA, most likely by forming mixed polymers (22–24). These truncated genes are also unable to confer ultraviolet resistance to *recA*⁻ bacteria, whereas truncations at residues 327 (23) or 335 (24) are able to confer such resistance.

The similar helical structures formed by the RAD51 and RecA proteins suggests that structure has been conserved more strongly than sequence in these prokaryotic and eukaryotic recombination proteins. The unusual structure of the DNA induced by both proteins and its role in homologous recognition and strand exchange should be examined. We recently determined that the UvsX protein of bacteriophage T4, which is even less homologous to RecA than is RAD51 (25), also induces this same DNA structure (26). The induction of a

similar DNA conformation, with a 5.1 Å rise per base pair and a 92 to 99 Å pitch, by all three of these proteins may not be epiphenomenal but may be a strong force in the conservation of this fundamental nucleoprotein structure. The recent finding of RAD51 homologs expressed in chicken (35) and in mouse and human cells (36) provides further evidence for the universality of this structure across all of biology.

REFERENCES AND NOTES

- C. M. Radding, *J. Biol. Chem.* **266**, 5355 (1991).
- S. C. West, *Annu. Rev. Biochem.* **61**, 603 (1992).
- A. I. Roca and M. M. Cox, *Crit. Rev. Biochem. Mol. Biol.* **25**, 415 (1990).
- S. C. Kowalczykowski, *Annu. Rev. Biophys. Biochem. Chem.* **20**, 539 (1991).
- E. H. Egelman, *Curr. Opin. Struct. Biol.*, **3**, 189 (1993); _____ and A. Stasiak, in press.
- A. Shinohara, H. Ogawa, T. Ogawa, *Cell* **69**, 457 (1992).
- _____, unpublished results.
- A. Stasiak, E. DiCapua, T. Koller, *J. Mol. Biol.* **151**, 557 (1981).
- D. J. DeRosier and P. B. Moore, *ibid.* **52**, 355 (1970).
- E. H. Egelman, *Ultramicroscopy* **19**, 367 (1986).
- E. DiCapua, A. Engel, A. Stasiak, T. Koller, *J. Mol. Biol.* **157**, 87 (1982).
- A. Stasiak and E. Di Capua, *Nature* **299**, 185 (1982).
- X. Yu and E. H. Egelman, *Biophys. J.* **57**, 555 (1990).
- R. M. Story, I. T. Weber, T. A. Steitz, *Nature* **355**, 318 (1992).
- X. Yu and E. H. Egelman, *J. Mol. Biol.* **227**, 334 (1992).
- E. H. Egelman and A. Stasiak, *ibid.* **191**, 677 (1986).
- D. K. Bishop, D. Park, L. Xu, N. Kleckner, *Cell* **69**, 439 (1992).
- J. R. Rusche, W. Konigsberg, P. Howard-Flanders, *J. Biol. Chem.* **260**, 949 (1985).
- R. C. Benedict and S. C. Kowalczykowski, *ibid.* **263**, 15513 (1988).
- S. Tateishi, T. Horii, T. Ogawa, H. Ogawa, *J. Mol. Biol.* **223**, 115 (1992).
- X. Yu and E. H. Egelman, *J. Struct. Biol.* **106**, 243 (1991).
- G. T. Yarranton and S. G. Sedgwick, *Mol. Gen. Genet.* **185**, 99 (1982).
- T. Horii, N. Ozawa, T. Ogawa, H. Ogawa, *J. Mol. Biol.* **223**, 105 (1992).
- F. Larminat and M. Defais, *Mol. Gen. Genet.* **216**, 106 (1989).
- H. Fujisawa, T. Yonesaki, T. Minagawa, *Nucleic Acids Res.* **13**, 7473 (1985).
- X. Yu and E. H. Egelman, *J. Mol. Biol.*, in press.
- P. L. Moreau and M.-F. Carlier, *J. Biol. Chem.* **264**, 2302 (1989).
- M. Adrian *et al.*, *Nature* **308**, 32 (1984).
- A reaction mixture ([RAD51], 6.5 μM; [DNA], 2 μM (bp); [ATP], 2.5 mM; [Mg acetate], 10 mM; all in 25 mM (pH 7.2) triethanolamine buffer) was incubated at 23°C for 1 hour, and then 2.5 mM NaF and 2.5 mM Al(NO₃)₃ were added and incubated at 23°C for an additional 30 min to form RAD51-DNA-adenosine diphosphate (ADP)-AlF₄⁻ filaments, where ADP-AlF₄⁻ is a stable analog for either ATP or ADP-inorganic phosphate (13, 27). The circular ΦX174 molecules were nicked with deoxyribonuclease I so that the RAD51 could completely cover the DNA without torsional stress, and the linear molecules were prepared by Pst I (IBI, New Haven, CT) cutting of the ΦX174. For negative staining, samples were prepared on carbon-coated grids that had been glow-discharged, blotted, and stained with 2% uranyl acetate. Frozen-hydrated specimens were prepared on a holey carbon film, rapidly frozen in a propane slush, and maintained at -170°C in a Gatan (Pleasanton, CA) 626 cold stage. All mi-

crographs were obtained on a JEOL (Tokyo, Japan) 1200EXII operating at 120 kV.

30. X. Yu and E. H. Egelman, *J. Mol. Biol.* **225**, 193 (1992).
31. C.-F. Chang *et al.*, *J. Ultrastruct. Mol. Struct. Res.* **100**, 166 (1988).
32. E. DiCapua *et al.*, *J. Mol. Biol.* **214**, 557 (1990).
33. Tilts of negatively stained filaments showed that the RAD51 one-start helix is right-handed as is RecA. Minimal-dose procedures were used to avoid excessive radiation damage. Layer lines were indexed as arising from a structure with a repeat of 37 subunits in six turns of a 99 Å pitch helix. The layer lines used for the RAD51 reconstruction were: $l = 0, n = 0$; $l = 1, n = -6$; $l = 5, n = 7$; $l = 6, n = 1$; $l = 7, n = -5$; and $l = 12, n = 2$. The RecA reconstruction had, in addition, $l = 13, n = -4$. The threshold density for both the surface views and the contour plots was chosen so that the appropriate molecular volume was contained, assuming a partial specific volume of $0.75 \text{ cm}^3 \text{ g}^{-1}$. For the RAD51 reconstruction, a molecular volume corresponding to 30 kD, rather than 43 kD, was used because 120 additional NH_2 -terminal residues were not visualized. The

use of a larger molecular volume leads to a nearly isotropic enlargement of the reconstruction. In a comparison of the two polymers, several observations suggest that the RAD51 filament is even less regular than the very flexible RecA filament, and a comparison of layer line data suggests that the resolution of the RAD51 reconstruction is lower than that of the comparable RecA reconstruction. The transform of the crystal structure C_α backbone was multiplied by a Gaussian filter having a standard deviation of $1/(30 \text{ \AA})$ and then back-transformed to match the electron microscopic resolution.

34. A. Stasiak, E. H. Egelman, P. Howard-Flanders, *J. Mol. Biol.* **202**, 659 (1988).
35. O. Bezzubova, A. Shinohara, R. G. Mueller, H. Ogawa, J.-M. Buerstedde, *Nucleic Acids Res.*, in press.
36. A. Shinohara *et al.*, unpublished results.
37. Supported by a grant-in-aid for Science Research on Priority Areas from the Ministry of Education, Science, and Culture of Japan and by U.S. NIH grant GM35269.

17 November 1992; accepted 11 February 1993

Antibody-Catalyzed Degradation of Cocaine

Donald W. Landry,* Kang Zhao,† Ginger X.-Q. Yang, Michael Glickman, Taxiarchis M. Georgiadis

Immunization with a phosphonate monoester transition-state analog of cocaine provided monoclonal antibodies capable of catalyzing the hydrolysis of the cocaine benzoyl ester group. An assay for the degradation of radiolabeled cocaine identified active enzymes. Benzoyl esterolysis yields ecgonine methyl ester and benzoic acid, fragments devoid of cocaine's stimulant activity. Passive immunization with such an artificial enzyme could provide a treatment for dependence by blunting reinforcement.

Addiction to cocaine afflicts Western populations in epidemic proportions, and the exceptional reinforcing effect of cocaine renders abuse of this stimulant most resistant to treatment (1). Cocaine reinforces self-administration in relation to the peak serum concentration of the drug, the rate of rise to the peak, and the degree of change of the serum level (2). The drug rapidly partitions from serum into the central nervous system (CNS) and binds specifically to reuptake carriers for several monoamine neurotransmitters (3). The function of these presynaptic transporters appears to be the inactivation of released neurotransmitter (4). The receptor that mediates the reinforcing effect of cocaine corresponds to its binding site for competitive inhibition of dopamine reuptake (5). This reuptake inhibition is hypothesized to potentiate dopaminergic neurotransmission in mesolimbocortical pathways and ultimately result in reinforcement (6). Direct antagonists of cocaine-induced reinforcement do not exist currently, and agents that promote abstinence, such as desipramine, have

an induction period of several weeks (7).

As an alternative to therapeutic approaches that are based on the pharmacology of the cocaine receptor, the delivery of cocaine to its receptor could be interrupted. Antibodies against opiates were found to antagonize the reinforcing effect of heroin in a paradigm of drug self-administration in a rhesus monkey (8). However, although successful in extinguishing heroin self-ad-

ministration at low doses of heroin, these antibodies failed for repetitive high doses because of the depletion of circulating antibody by complex formation.

The recent development of catalytic antibodies (9) provides a potential solution to the problem of antibody depletion. Immunization with a stable analog of the evanescent transition-state structure of a chemical reaction can yield monoclonal antibodies with the capacity to catalyze the modeled reaction (10). A catalytic antibody could bind the target substrate, catalyze a deactivating transformation, and release the inactive products, and the antibody would be free for further binding.

Of all the commonly abused substances, cocaine is the best candidate for the catalytic-antibody approach. Hydrolysis of cocaine's benzoyl ester by a catalytic antibody would yield ecgonine methyl ester and benzoic acid, fragments that retain none of cocaine's stimulant or reinforcing activities (11). Antibodies with esterase activity approaching that of natural enzymes have been reported (10, 12), and cocaine's benzoyl ester side group, with its large hydrophobic surface, is particularly suited to elicit antibodies with strong binding and catalytic activity.

The transition state of the benzoyl ester cleavage reaction probably resembles the tetrahedral intermediate of second-order ester hydrolysis (13) and can be stably mimicked in terms of geometry and charge distribution by a suitably designed phosphonate monoester (9, 14) (Fig. 1). Transition-state analogs based on the phosphonate monoester functional group have yielded artificial esterases with the highest activities (10, 12); but these analogs can idiosyncratically fail to elicit catalytically active antibodies, and so the rules for analog construction must be empirically defined (15). Recently, investigators have described strategies to increase the frequency of obtaining enzymatic antibodies, such as the "bait and switch" (16) and substrate-attenuation (15) techniques. However, these approaches

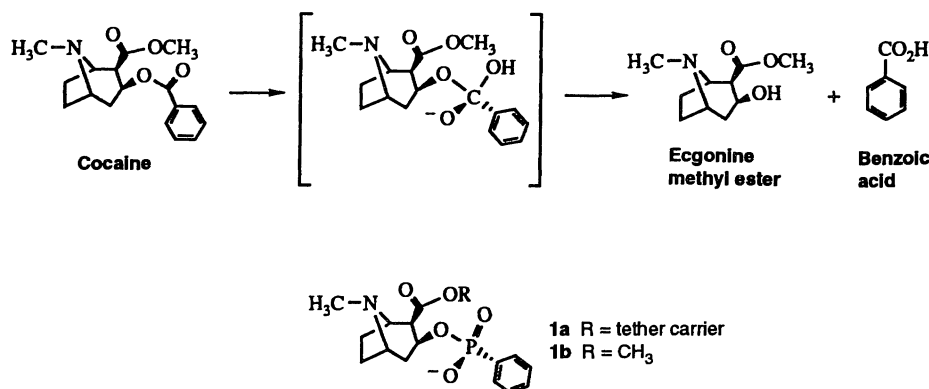


Fig. 1. Hydrolysis of the benzoyl ester of cocaine. Presumed tetrahedral intermediate formed along the reaction pathway is shown in brackets. General structure of a phosphonate monoester analog of the benzoyl ester is pictured immediately below the intermediate. The R substituent for **1a** is the tether depicted in Fig. 2.

Department of Medicine, Columbia University College of Physicians and Surgeons, New York, NY 10032.

*To whom correspondence should be addressed.

†Present address: Department of Chemistry, New York University, New York, NY 10003.